Complexed crystal structure of SSB reveals a novel single-stranded DNA binding mode (SSB)$_{3:1}$: Phe60 is not crucial for defining binding paths

Yen-Hua Huang [a], En-Shyh Lin [b], Cheng-Yang Huang [a, c, *]

[a] School of Biomedical Sciences, Chung Shan Medical University, No.110, Sec.1, Chien-Kuo N. Rd., Taichung City, Taiwan
[b] Department of Beauty Science, National Taichung University of Science and Technology, No.193, Sec.1, San-Min Rd., Taichung City, Taiwan
[c] Department of Medical Research, Chung Shan Medical University Hospital, No.110, Sec.1, Chien-Kuo N. Rd., Taichung City, Taiwan

ARTICLE INFO

ABSTRACT

Single-stranded DNA-binding protein (SSB) is essential to cells as it participates in DNA metabolic processes, such as DNA replication, repair, and recombination. *Escherichia coli* SSB (EcSSB) tetramer cooperatively binds and wraps ssDNA in two major binding modes. In this study, we report the complex crystal structure of *Pseudomonas aeruginosa* SSB (PaSSB) with ssDNA dT20 at 2.39 Å resolution (PDB entry 6JDG) that revealed a new binding mode, namely, (SSB)$_{3:1}$. In the (SSB)$_{65}$ mode revealed by the EcSSB −dC35 complex structure, all four subunits fully participate in the binding to ssDNA. However, only three subunits in the PaSSB tetramer can participate in wrapping ssDNA in the (SSB)$_{3:1}$ mode. The bound ssDNA in the PaSSB−ssDNA complex adopts an Ω-shaped conformation rather than a χ−shaped conformation in the (SSB)$_{65}$ mode possibly due to the disability of Phe60. Phe60 is known to play a critical role in defining DNA-binding paths and promoting the wrapping of ssDNA around SSB tetramers. However, it is not important in the (SSB)$_{3:1}$ mode. The ssDNA binding path revealed by our structural evidence suggests that ssDNA occupies half of the binding sites of the two subunits and slightly comes into contact with the ssDNA binding sites of the third subunit. Accordingly, we propose and sketch a possible wrapping mechanism of SSB via this novel ssDNA-binding mode, (SSB)$_{3:1}$.

© 2019 Elsevier Inc. All rights reserved.

1. Introduction

Single-stranded DNA-binding proteins (SSBs) are ubiquitous within all kingdoms of life and play essential roles in DNA replication, recombination, repair, and replication restart [1–3]. SSB is required to maintain the transient unwinding of duplex DNA in a single-stranded state. SSB exhibits high affinity for ssDNA with no considerable sequence specificity. Bacterial SSB consists of an N-terminal ssDNA-binding domain and a flexible C-terminal protein−protein interaction domain [4]. The N-terminal domain consists of an oligosaccharide/oligonucleotide-binding (OB) fold [5]. SSB binds to many nucleoproteins and enzymes associated with DNA metabolism that constitute the SSB interactome [4,6]. SSB recruits these nucleoproteins, such as PriA [7–9], exonuclease I

[10], RecA [11], RecG [12], RecO [13], and RecQ [14], and stimulates their activities. However, given their inherent differences, some Gram-positive bacterial SSBs such as *Bacillus subtilis* SsbA [15], *Staphylococcus aureus* SsbA [16], SsbB [17], and SsbC [18], do not activate PriA helicase. A long glycine-rich hinge known as the intrinsically disordered linker (IDL) in the C-terminal domain of SSB is also involved in mediating the binding of partner proteins [19–21]. The entire C-terminal domain of SSB is disordered even in the presence of ssDNA [22].

The structure, DNA binding properties, and functions of SSB in *Escherichia coli* (EcSSB) have been studied extensively [2–4]. EcSSB forms a stable homotetramer, which binds and wraps ssDNA around its subunit [23]. EcSSB tetramer cooperatively binds and wraps ssDNA in two major binding modes [24]. These two distinct binding modes are dependent on salt concentration in a solution [24]. In the (SSB)$_{35}$ binding mode, which is favored in low salt concentrations (<10 mM NaCl), only two subunits in an EcSSB tetramer bind 35 nts to form the SSB$_{35}$ complex. In the (SSB)$_{65}$ binding mode, which is favored in moderately high salt
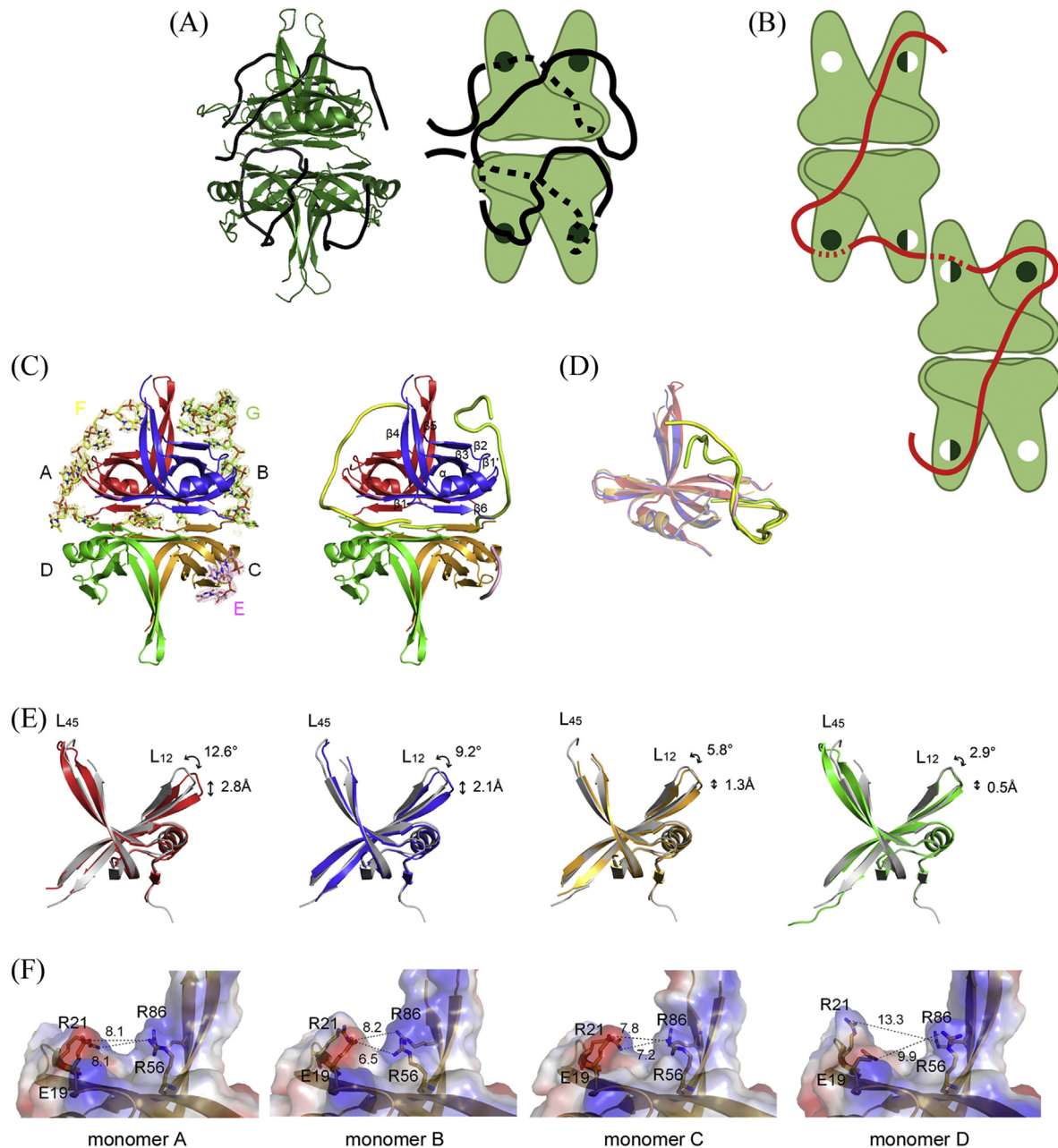
Fig. 1. Structure and binding modes of SSB. (A) The (SSB)$_{65}$ mode (PDB entry 1EYG). All four subunits of EcSSB (forest) participate in the binding to ssDNA (black). ssDNA that passes along the backside of the schematic is depicted as a dotted line. OB-fold binding sites are represented with either an open circle, for an unoccupied binding site; a half-closed circled, for a partially occupied binding site; or a closed circle, for a fully occupied binding site [26]. (B) The (SSB)$_{35}$ mode. ssDNA (red) comes into full contact with one subunit and only partially contacts with two other subunits for an average of two OB domains per SSB homotetramer. (C) Crystal structure of PaSSB complexed with ssDNA dT20. Four monomers of PaSSB (monomers A, B, C, and D) and three ssDNAs (chains E, F, and G) were found in the asymmetric unit. The composite omit map (at 1.0 σ) indicated the presence of ssDNA. (D) The superimposed structures of monomer A, B, and C revealed that the ssDNA binding modes in each monomer are different. (E) Conformational differences between the apo and dT20-bound form of PaSSB. Relative to their positions in apo-PaSSB (gray), the L$_{12}$ loop in monomers A (red), B (blue), C (orange), and D (green) in the complex structure of PaSSB was shifted by angles of 12.6°, 9.2°, 5.8°, and 2.9° and distances of 2.8, 2.1, 1.3, and 0.5 Å, respectively. (F) The ssDNA interaction cavity. The ssDNA interaction cavity created by residues E19 (β1′), R21 (β1′), R56 (β3), and R86 (β4) in monomer D (the unbound state) was wider than that in monomers A, B, and C. (For interpretation of the references to colour in this figure legend, the reader is referred to the Web version of this article.)

concentrations (>200 mM NaCl), all four subunits of EcSSB participate in ssDNA binding to form the SSB$_{65}$ complex. Intermediate ssDNA binding states of EcSSB are also found via structural changes between the SSB$_{35}$ and SSB$_{65}$ complexes [25]. During the different stages of DNA metabolism, different binding modes of SSB to ssDNA may be required for in vivo function [26,27].

Crystallographic studies of SSB bound with two molecules of 35-mer ssDNA determined to a resolution of 2.8 Å suggest a model for the SSB$_{65}$ complex [23]. Given that protein crystallization usually occurs at high salt conditions, the crystal structure for describing the (SSB)$_{35}$ mode that is used for the ssDNA binding of SSB at low salt conditions (<10 mM NaCl) is not easily obtained by X-ray chromatographic analysis. Complexed crystal structures of SSB are needed to understand how SSB can stably bind ssDNA in different and intermediate wrapping states.

In this study, we report the complex crystal structure of

Pseudomonas aeruginosa SSB (PaSSB) with ssDNA dT20 at 2.39 Å resolution (PDB entry 6JDG) that revealed a novel binding mode, namely, $(SSB)_{3:1}$. Unlike the $(SSB)_{65}$ mode showing all four subunits that fully participate in the binding to ssDNA, only three subunits in the PaSSB tetramer can participate in wrapping ssDNA in the $(SSB)_{3:1}$ mode. In addition, we find that the bound ssDNA in the PaSSB−ssDNA complex adopts an Ω-shaped conformation rather than a χ-shaped conformation in the $(SSB)_{65}$ mode. On the basis of structural evidence, we propose and sketch a possible wrapping mechanism of SSB via this novel ssDNA-binding mode, $(SSB)_{3:1}$.

2. Materials and methods

2.1. Protein expression and purification

Construction of the PaSSB expression plasmid has been reported [20,28,29]. The recombinant PaSSB protein was purified using the protocol described previously for SSB-like proteins [8,30]. Briefly, *E. coli* BL21(DE3) cells transformed with the expression vector were grown at 37 °C in LB medium supplemented with 100 µg/mL ampicillin. PaSSB expression was induced by incubating with 1 mM isopropyl thiogalactopyranoside. PaSSB was purified from the soluble supernatant by Ni^{2+}-affinity chromatography (HiTrap HP; GE Healthcare Bio-Sciences), eluted with Buffer A (20 mM Tris-HCl, 250 mM imidazole, and 0.5 M NaCl, pH 7.9), and dialyzed against a dialysis buffer (20 mM HEPES and 100 mM NaCl, pH 7.0; Buffer B). Protein purity remained at >97% as determined by SDS-PAGE.

2.2. Crystallography

Before crystallization, PaSSB was concentrated to 20 mg/mL in Buffer B. PaSSB was incubated with dT20 at a 1:4 (PaSSB tetramer/dT20) ratio. Crystals were grown at room temperature by hanging drop vapor diffusion in 10% PEG 8000 and 200 mM magnesium acetate. Diffraction data were collected using an ADSC Quantum-315r CCD area detector at SPXF beamline BL13C1 at NSRRC (Taiwan). All data integration and scaling were carried out using HKL-2000 [31]. The crystal structure of PaSSB complexed with ssDNA dT20 was determined at 2.39 Å resolution with the molecular replacement software Phaser-MR [32] using PaSSB as model (PDB entry 5YUO) [20]. Four monomers of PaSSB (monomers A, B, C and D) and three ssDNAs (chains E, F and G) were found per asymmetric unit. A model was built and refined with PHENIX [33] and Coot [34]. The final structure was refined to an *R*-factor of 0.213 and an R_{free} of 0.264. Atomic coordinates and related structure factors have been deposited in the PDB with accession code 6JDG.

3. Results and discussion

3.1. Overall structure of PaSSB tetramer with ssDNA dT20

EcSSB tetramer binds DNA in two major binding modes [24]. In the $(SSB)_{65}$ mode (Fig. 1A), as revealed by the EcSSB−dC35 complex structure [23], all four subunits participate in the binding to ssDNA. In the $(SSB)_{35}$ mode (Fig. 1B), ssDNA comes into full contact with one subunit and only partially contacts with two other subunits for an average of two OB domains per SSB homotetramer [25,26]. However, no such complexed structure is available. In this study, we solved the crystal structure of PaSSB complexed with ssDNA dT20 at 2.39 Å resolution (Table 1) and found a new ssDNA interaction mode, namely, $(SSB)_{3:1}$ (Fig. 1C). This mode is similar to but different from the $(SSB)_{35}$ mode. Four monomers of PaSSB (monomers A, B, C, and D) and three ssDNAs (chains E, F, and G) were found in the asymmetric unit. Similar to the apo-PaSSB structure [20], the PaSSB monomer in this complex structure has

three pairs of antiparallel β-strands (β1′β2, β2β3, β4β5) and folds as an OB-fold, with the core bearing β-barrel capped by an α-helix (Fig. 1C). The ssDNA interaction sites in each monomer are different (Fig. 1D). Through the superimposed structures, conformational differences between the apo and dT20-bound form of PaSSB were mainly observed in the L_{12} and L_{45} loops (Fig. 1E). Relative to their positions in apo-PaSSB (gray), the L_{12} loop in monomers A (red), B (blue), C (orange), and D (green) in the complex structure of PaSSB was shifted by angles of 12.6°, 9.2°, 5.8°, and 2.9° and distances of 2.8, 2.1, 1.3, and 0.5 Å, respectively. The ssDNA interaction cavity created by residues E19 (β1′), R21 (β1′), R56 (β3), and R86 (β4) in monomer D (the unbound state) was wider than that in monomers A, B, and C (Fig. 1F). Compared with the structure of apo-PaSSB [20], the conformation of monomer D in this complex structure did not significantly differ in terms of position.

SSBs do not limit the conformation of bound ssDNA [35]; thus, the largely unstructured ssDNA can slide freely through the ssDNA binding domain of SSB [36]. Consequently, this high ssDNA mobility causes the bound DNAs to be disordered and non-visible in the electron density map [35]. Although we used dT20 for crystal growth, continuous electron density was observed only for nucleotides T7−9 in chain E (3 mers); T4−12 and T15−16 in chain F (11 mers); and T2−12, T15, and T17 in chain G (13 mers). For clarity, undefined T13 and T14 in chain F and T16 in chain G were modeled (Fig. 1C). Similar to that of EcSSB [22], the entire C-terminal domain of PaSSB (aa 116−165) is disordered and disappears even when bound to ssDNA.

3.2. ssDNA interaction sites

The protein−ssDNA interface reveals an extensive network of interactions that involves the stacking of aromatic side chains with DNA bases and a number of hydrogen bonds and electrostatic

Table 1
Data collection and refinement statistics.

Data collection	
Crystal	PaSSB−dT20
Wavelength (Å)	0.975
Resolution (Å)	30−2.39
Space group	$P3_1$
Cell parameters	
a, b, c (Å)	60.04, 60.04, 129.64
α, β, γ (°)	90, 90, 120
Completeness (%)[a]	99 (99.8)*
<I/σI>	20.27 (2.4)
R_{sym} or R_{merge} (%)[b]	0.049 (0.463)
Redundancy	3.1 (3.2)
Refinement	
Resolution (Å)	29.25−2.39
No. reflections	20581
R_{work}/R_{free}	0.213/0.264
No. atoms	
Protein	400
DNA	27
Water	25
Ratio (polypeptide chain: ssDNA)	4:3
R.m.s deviation	
Bond lengths (Å)	0.009
Bond angles (°)	0.996
Ramachandran Plot	
In preferred regions	369 (97.11%)
In allowed regions	11 (2.89%)
Outliers	0 (0%)
PDB entry	6JDG

[a] Values in parentheses are for the highest resolution shell.
[b] $R_{sym} = \Sigma|I − \text{'I'}|/\Sigma I$, where I is the observed intensity, 'I' is the statistically weighted average intensity of multiple observations of symmetry-related reflections.
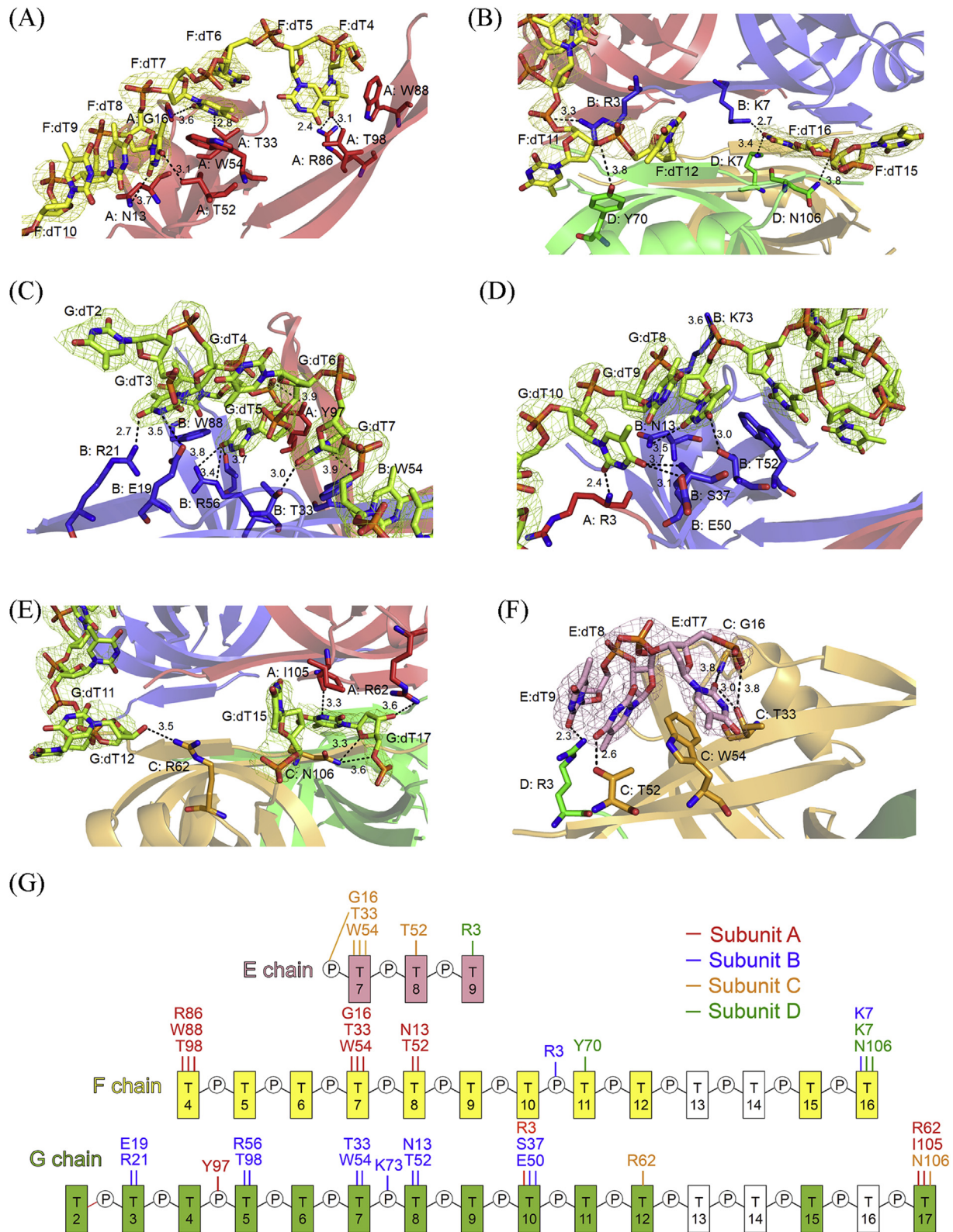
Fig. 2. ssDNA interaction sites. A detailed view of the PaSSB–ssDNA interactions for (A) T4–10 in chain F, (B) T11–12 and T15–16 in chain F, (C) T2–7 in chain G, (D) T8–10 in chain G, (E) T11–12, T15, and T17 in chain G, and (F) T7–9 in chain E is shown. (G) A schematic diagram of the protein–ssDNA interactions in the PaSSB–dT20 complex.

interactions between the PaSSB tetramer and the three ssDNA homopolymers (Fig. 2). Given that ssDNA does not completely come into contact with all four subunits of PaSSB, the ssDNA interaction sites in each monomer are different. A detailed view of

the PaSSB–ssDNA interactions for T4–10 (Fig. 2A), T11–12 (Fig. 2B), and T15–16 (Fig. 2B) in chain F; T2–7 (Fig. 2C), T8–10 (Fig. 2D), T11–12 (Fig. 2E), T15 (Fig. 2E), and T17 (Fig. 2E) in chain G; and T7–9 in chain E (Fig. 2F) is shown. A schematic diagram of the
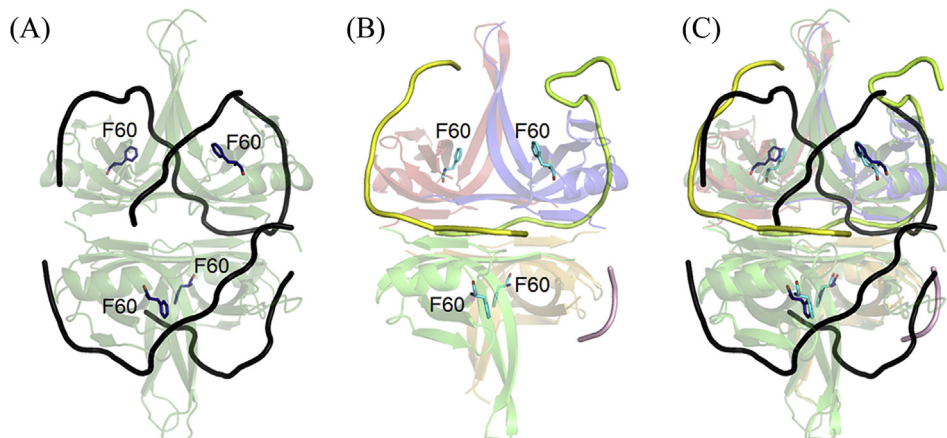
Fig. 3. Phe60 is not crucial for ssDNA binding. (A) The EcSSB−dC35 complex. All four Phe60 of the SSB tetramer on the DNA binding surface make stacking interactions with the ssDNA and guide ssDNA wrapping for the (SSB)$_{65}$ mode [23]. (B) The PaSSB−dT20 complex. Unlike that in the EcSSB−dC35 complex, the location of Phe60 in the PaSSB−dT20 complex is too far away for it to interact with ssDNA. (C) The superimposed structures of the EcSSB−dC35 and the PaSSB−dT20 complex.

protein−ssDNA interactions in the PaSSB−dT20 complex is also shown in Fig. 2G. Structurally, Arg3 (in monomers A, B, and D), Lys7 (B, D), Asn13 (A, B), Gly15 (A, C), Glu19 (B), Arg21 (B), Thr33 (A, B, C), Ser37 (B), Glu50 (B), Thr52 (A, B, C), Trp54 (A, B, C), Arg56 (B), Arg62 (A, C), Tyr70 (D), Lys73 (B), Arg86 (A), Trp88 (A), Tyr97 (A), Thr98 (A, B), Ile105 (A), and Asn106 (C, D) were involved in ssDNA binding. Lys7 and Arg62 are also crucial for interacting with inhibitor myricetin [37].

3.3. Phe60 is not crucial for ssDNA binding

The highly conserved Phe60 is known to play a critical role in defining DNA binding paths and promoting the wrapping of ssDNA around SSB tetramers (Fig. 3A) [4,23]. In the EcSSB−dC35 complex, all four Phe60 of the SSB tetramer on the DNA binding surface make stacking interactions with the ssDNA and guide ssDNA wrapping for the (SSB)$_{65}$ mode [23]. In the PaSSB−dT20 structure, however, we did not find any role in the ssDNA binding of any Phe60 in all four subunits of PaSSB (Fig. 3B and C). Unlike that in the EcSSB−dC35 complex, the location of Phe60 in the PaSSB−dT20 complex is too far away for it to interact with ssDNA. The distance between Phe60 and the nearest ssDNA is 11.2 Å (monomer A and

chain F), 13.3 Å (monomer B and chain G), and 18.2 Å (monomer C and chain E). These distances suggest no interaction. Thus, Phe60 is not crucial for ssDNA binding and does not play a role in part or in entirety in defining the DNA binding paths of SSB.

3.4. Novel ssDNA binding mode (SSB)$_{3:1}$

Given that protein crystallization usually occurs at high salt conditions, the crystal structure for the (SSB)$_{35}$ mode used for the ssDNA binding of SSB at low salt conditions cannot be easily obtained by X-ray chromatographic analysis. Although SSB cooperatively binds ssDNA [24], our structural evidence for the (SSB)$_{3:1}$ mode revealed that the ssDNA interaction cavity in monomer D is not a preferred site for ssDNA binding (Fig. 1C). This situation is remarkably different from the (SSB)$_{65}$ mode but somehow similar to the (SSB)$_{35}$ mode (Fig. 1B). The clamp in monomer D of PaSSB has a "closed" conformation (Fig. 1F) and affects the topology of the DNA binding surface (Fig. 4A). In addition, Phe60, the important aromatic residue for the ssDNA binding of EcSSB [23], does not interact with ssDNA in the complex crystal structure of PaSSB (Fig. 3B). Consequently, these significant differences may explain why distinct ssDNA binding mechanisms can be used for SSBs.
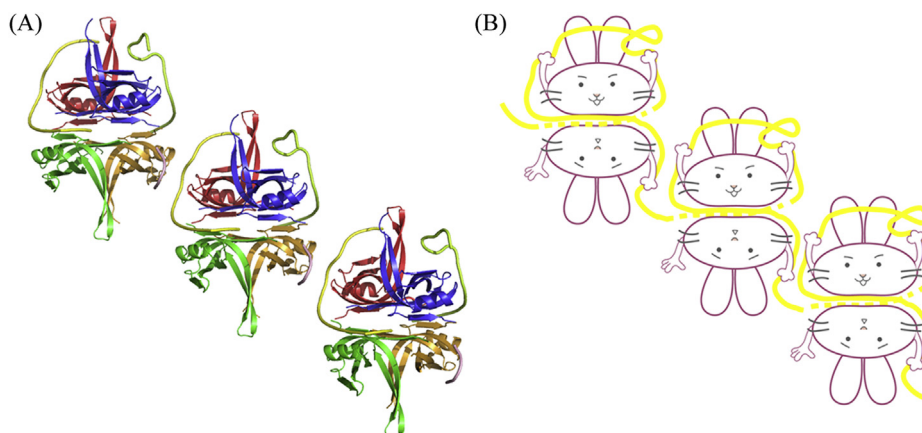

Fig. 4. Possible wrapping mechanism of SSB via the (SSB)$_{3:1}$ mode. (A) The symmetry-related structures of the PaSSB−dT20 complex. (B) A cartoon model. Our complex structure of PaSSB−dT20 reveals that only three and not all four subunits can participate in wrapping around ssDNA in the (SSB)$_{3:1}$ mode. In addition, the ssDNA interaction cavity in monomer D is not a preferred site for ssDNA binding. The bound ssDNA in the PaSSB−ssDNA complex adopts an Ω-shaped conformation rather than a χ-shaped conformation possibly due to the disability of Phe60. This ssDNA binding mode (SSB)$_{3:1}$ revealed by the complex structure differs significantly from (SSB)$_{65}$. Basing from these results, we proposed a cartoon model to show possible wrapping mechanism of SSB via the (SSB)$_{3:1}$ mode.

3.5. Possible wrapping mechanism of SSB via the (SSB)$_{3:1}$ mode

A model for the (SSB)$_{3:1}$ mode can be postulated on the basis of the complex structure of PaSSB by using the symmetry-related complexes generated along the L$_{12}$ loops. The symmetry-related complex structures reveal one path by which a long, continuous stretch of ssDNA can interact with adjacent SSB dimers (monomers A and B) to form an ssDNA-bound filament of PaSSB (Fig. 4A). Unlike the bound dC35 in the EcSSB–dC35 complex adopting a χ-shaped conformation (Fig. 1A), the bound dT20 in the PaSSB–dT20 complex adopts an Ω-shaped conformation that is majorly defined by monomers A and B (Fig. 1C). Given the lack of contribution of Phe60 (Fig. 3), ssDNA does not occupy the entire binding sites and are not fully wrapped around each PaSSB subunit. Thus, the ssDNA binding path revealed by our in silico experiment suggests that ssDNA occupies half of the binding sites of two subunits (monomers A and B) and only slightly contacts the ssDNA binding site of the third subunit (monomer C). Furthermore, ssDNA does not occupy the ssDNA binding site of the fourth subunit (monomer D). Given the structural evidence, we propose a possible wrapping mechanism of SSB tetramers via the (SSB)$_{3:1}$ mode, as shown in Fig. 4B.

In conclusion, our complex structure of PaSSB–dT20 reveals that only three and not all four subunits, namely, monomers A, B, and C in the SSB tetramer, can participate in wrapping around ssDNA in the (SSB)$_{3:1}$ mode. In addition, the bound ssDNA in the PaSSB–ssDNA complex adopts an Ω-shaped conformation rather than a χ-shaped conformation possibly due to the disability of Phe60. This ssDNA binding mode (SSB)$_{3:1}$ revealed by the complex structure differs significantly from (SSB)$_{65}$.

Acknowledgments

Transparency document

Transparency document related to this article can be found online at https://doi.org/10.1016/j.bbrc.2019.10.036.

References

[1] T.A. Windgassen, S.R. Wessel, B. Bhattacharyya, J.L. Keck, Mechanisms of bacterial DNA replication restart, Nucleic Acids Res. 46 (2018) 504—519.

[2] E. Antony, T.M. Lohman, Dynamics of E. coli single stranded DNA binding (SSB) protein-DNA complexes, Semin. Cell Dev. Biol. 86 (2019) 102—111.

[3] R.R. Meyer, P.S. Laine, The single-stranded DNA-binding protein of Escherichia coli, Microbiol. Rev. 54 (1990) 342—380.

[4] R.D. Shereda, A.G. Kozlov, T.M. Lohman, M.M. Cox, J.L. Keck, SSB as an organizer/mobilizer of genome maintenance complexes, Crit. Rev. Biochem. Mol. Biol. 43 (2008) 289—318.

[5] T.H. Dickey, S.E. Altschuler, D.S. Wuttke, Single-stranded DNA-binding proteins: multiple domains for multiple functions, Structure 21 (2013) 1074—1084.

[6] P.R. Bianco, The tale of SSB, Prog. Biophys. Mol. Biol. 127 (2017) 111—118.

[7] T.A. Windgassen, M. Leroux, K.A. Satyshur, S.J. Sandler, J.L. Keck, Structure-specific DNA replication-fork recognition directs helicase and replication restart activities of the PriA helicase, Proc. Natl. Acad. Sci. U. S. A 115 (2018) E9075—E9084.

[8] Y.H. Huang, Y. Lien, C.C. Huang, C.Y. Huang, Characterization of Staphylococcus aureus primosomal DnaD protein: highly conserved C-terminal region is crucial for ssDNA and PriA helicase binding but not for DnaA protein-binding and self-tetramerization, PLoS One 11 (2016), e0157593.

[9] C.J. Cadman, P. McGlynn, PriA helicase and SSB interact physically and functionally, Nucleic Acids Res. 32 (2004) 6378—6387.

[10] D. Lu, J.L. Keck, Structural basis of Escherichia coli single-stranded DNA-binding protein stimulation of exonuclease I, Proc. Natl. Acad. Sci. U. S. A 105 (2008) 9169—9174.

[11] R. Roy, A.G. Kozlov, T.M. Lohman, T. Ha, SSB protein diffusion on single-stranded DNA stimulates RecA filament formation, Nature 461 (2009) 1092—1097.

[12] Z. Sun, H.Y. Tan, P.R. Bianco, Y.L. Lyubchenko, Remodeling of RecG helicase at the DNA replication fork by SSB protein, Sci. Rep. 5 (2015) 9625.

[13] J. Inoue, T. Nagae, M. Mishima, Y. Ito, T. Shibata, T. Mikawa, A mechanism for single-stranded DNA-binding protein (SSB) displacement from single-stranded DNA upon SSB-RecO interaction, J. Biol. Chem. 286 (2011) 6720—6732.

[14] R.D. Shereda, D.A. Bernstein, J.L. Keck, A central role for SSB in Escherichia coli RecQ DNA helicase function, J. Biol. Chem. 282 (2007) 19247—19258.

[15] P. Polard, S. Marsin, S. McGovern, M. Velten, D.B. Wigley, S.D. Ehrlich, C. Bruand, Restart of DNA replication in Gram-positive bacteria: functional characterisation of the Bacillus subtilis PriA initiator, Nucleic Acids Res. 30 (2002) 1593—1605.

[16] Y.H. Huang, H.H. Guan, C.J. Chen, C.Y. Huang, Staphylococcus aureus single-stranded DNA-binding protein SsbA can bind but cannot stimulate PriA helicase, PLoS One 12 (2017), e0182060.

[17] K.L. Chen, J.H. Cheng, C.Y. Lin, Y.H. Huang, C.Y. Huang, Characterization of single-stranded DNA-binding protein SsbB from Staphylococcus aureus: SsbB cannot stimulate PriA helicase, RSC Adv. 8 (2018) 28367—28375.

[18] Y.H. Huang, C.Y. Huang, SAAV2152 is a single-stranded DNA binding protein: the third SSB in Staphylococcus aureus, Oncotarget 9 (2018) 20239—20254.

[19] R. Nigam, M. Mohan, G. Shivange, P.K. Dewangan, R. Anindya, Escherichia coli AlkB interacts with single-stranded DNA binding protein SSB by an intrinsically disordered region of SSB, Mol. Biol. Rep. 45 (2018) 865—870.

[20] Y.H. Huang, C.Y. Huang, The glycine-rich flexible region in SSB is crucial for PriA stimulation, RSC Adv. 8 (2018) 35280—35288.

[21] P.R. Bianco, S. Pottinger, H.Y. Tan, T. Nguyenduc, K. Rex, U. Varshney, The IDL of E. coli SSB links ssDNA and protein binding by mediating protein-protein interactions, Protein Sci. 26 (2017) 227—241.

[22] S.N. Savvides, S. Raghunathan, K. Futterer, A.G. Kozlov, T.M. Lohman, G. Waksman, The C-terminal domain of full-length E. coli SSB is disordered even when bound to DNA, Protein Sci. 13 (2004) 1942—1947.

[23] S. Raghunathan, A.G. Kozlov, T.M. Lohman, G. Waksman, Structure of the DNA binding domain of E. coli SSB bound to ssDNA, Nat. Struct. Biol. 7 (2000) 648—652.

[24] T.M. Lohman, M.E. Ferrari, Escherichia coli single-stranded DNA-binding protein: multiple DNA-binding modes and cooperativities, Annu. Rev. Biochem. 63 (1994) 527—570.

[25] S. Suksombat, R. Khafizov, A.G. Kozlov, T.M. Lohman, Y.R. Chemla, Structural dynamics of E. coli single-stranded DNA binding protein reveal DNA wrapping and unwrapping pathways, elife 4 (2015), e08193.

[26] V.M. Waldman, E. Weiland, A.G. Kozlov, T.M. Lohman, Is a fully wrapped SSB-DNA complex essential for Escherichia coli survival? Nucleic Acids Res. 44 (2016) 4317—4329.

[27] R. Roy, A.G. Kozlov, T.M. Lohman, T. Ha, Dynamic structural rearrangements between DNA binding modes of E. coli SSB protein, J. Mol. Biol. 369 (2007) 1244—1257.

[28] Y.H. Huang, C.Y. Huang, C-terminal domain swapping of SSB changes the size of the ssDNA binding site, BioMed Res. Int. 2014 (2014) 573936.

[29] H.C. Jan, Y.L. Lee, C.Y. Huang, Characterization of a single-stranded DNA-binding protein from Pseudomonas aeruginosa PAO1, Protein J. 30 (2011) 20—26.

[30] C.Y. Huang, C.H. Hsu, Y.J. Sun, H.N. Wu, C.D. Hsiao, Complexed crystal structure of replication restart primosome protein PriB reveals a novel single-stranded DNA-binding mode, Nucleic Acids Res. 34 (2006) 3878—3886.

[31] Z. Otwinowski, W. Minor, Processing of X-ray diffraction data collected in oscillation mode, Methods Enzymol. 276 (1997) 307—326.

[32] A.J. McCoy, R.W. Grosse-Kunstleve, P.D. Adams, M.D. Winn, L.C. Storoni, R.J. Read, Phaser crystallographic software, J. Appl. Crystallogr. 40 (2007) 658—674.

[33] J.J. Headd, N. Echols, P.V. Afonine, R.W. Grosse-Kunstleve, V.B. Chen, N.W. Moriarty, D.C. Richardson, J.S. Richardson, P.D. Adams, Use of knowledge-based restraints in phenix.refine to improve macromolecular refinement at low resolution, Acta Crystallogr. D Biol. Crystallogr. 68 (2012) 381—390.

[34] P. Emsley, K. Cowtan, Coot: model-building tools for molecular graphics, Acta Crystallogr. D Biol. Crystallogr. 60 (2004) 2126—2132.

[35] Y. Shamoo, A.M. Friedman, M.R. Parsons, W.H. Konigsberg, T.A. Steitz, Crystal structure of a replication fork single-stranded DNA binding protein (T4 gp32) complexed to DNA, Nature 376 (1995) 362—366.

[36] R. Romer, U. Schomburg, G. Krauss, G. Maass, Escherichia coli single-stranded DNA binding protein is mobile on DNA: ^{1}H NMR study of its interaction with oligo- and polynucleotides, Biochemistry 23 (1984) 6132—6137.

[37] C.Y. Huang, Crystal structure of SSB complexed with inhibitor myricetin, Biochem. Biophys. Res. Commun. 504 (2018) 704—708.